Spectroscopic Characterization of Ti Sites in MWW Zeolite in Presence of Hydrogen Peroxide

ChemCatChem

Supporting Information

Spectroscopic Characterization of Ti Sites in MWW Zeolite in Presence of Hydrogen Peroxide

Francesca Rosso, Alessia Airi, Matteo Signorile, Silvia Bordiga, Valentina Crocellà, and Francesca Bonino*

Electronic Supplementary Information

Spectroscopic Characterization of Ti Sites in MWW Zeolite in Presence of Hydrogen Peroxide

Francesca Rosso[a], Alessia Airi[a], Matteo Signorile[a], Silvia Bordiga[a], Valentina Crocellà[a], Francesca Bonino[a,*]

a Department of Chemistry, NIS and INSTM Reference Centre, Università di Torino, Via G. Quarello 15, 10135 and Via P. Giuria 7, 10125, Torino, Italy.

* Corresponding author.

E-mail address: francesca.bonino@unito.it (Francesca Bonino)

Crystalline Structure and Defects Analysis

Figure S1 shows the InfraRed (IR) spectra recorded in transmission, on the pelletized samples, after 20 min of outgassing at Room Temperature (RT), using the set-up described for the sake of IR experiments with probe molecules (Characterization Techniques paragraph in the main text).

The spectra show the typical signals of the zeolite, overlapped to those of the Organic Structure Directing Agent (OSDA) molecules trapped in the pores. At 3745 cm^{-1} a very weak and a weak signals are visible in Ti-MWW-as and Ti-MWW-HNO_3-as respectively, assigned to isolated silanol (Si-OH) groups present on the surface of the zeolite. The signals between 3000 and 2800 cm^{-1} are assigned to the C-H stretching mode bands, while the 1500-1250 cm^{-1} spectral range hosts the C-H bending and deformation mode bands due to the presence of the two OSDA molecules. Detailed assignment can be found elsewhere.[1] Since the spectra are internally normalized to the Si-O-Si overtone absorptions, the intensity of the signals can be quantitatively compared. This suggests that the amount of organic molecules trapped in the pores in Ti-MWW-HNO_3-as is lower respect to the amount present before the acid washing.

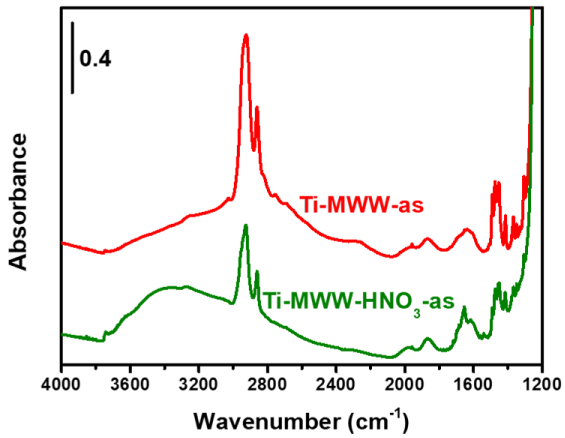

Figure S1. Vertically shifted IR spectra of, from bottom to top, Ti-MWW-HNO_3-as and Ti-MWW-as after 20 min of outgassing at RT, internally normalized at the Si-O-Si stretching overtone absorptions and vertically shifted for the sake of comparison.

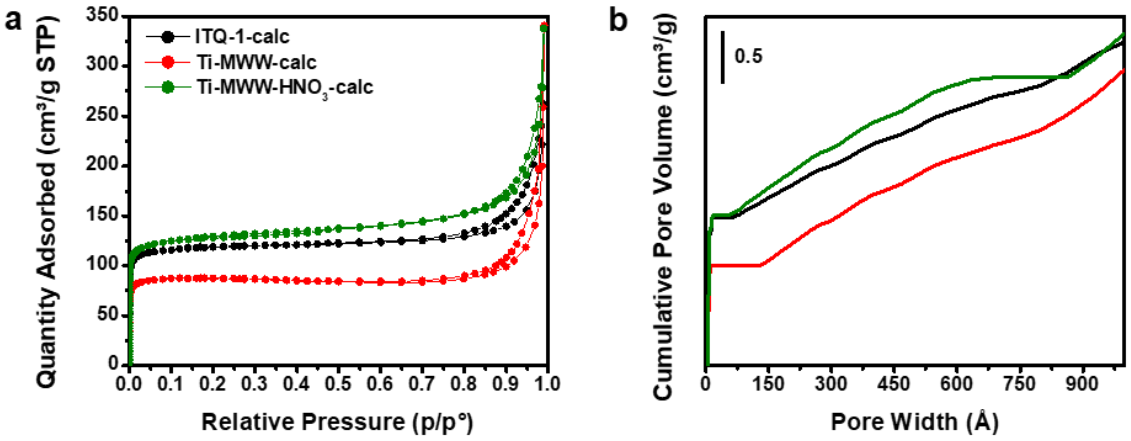

Figure S2. (a) Volumetric N_2 adsorption/desorption isotherms at -196 °C in the whole relative pressure range and (b) cumulative pore volume plot in the 0 – 1000 Å pore size range, obtained applying the NL-DFT model.

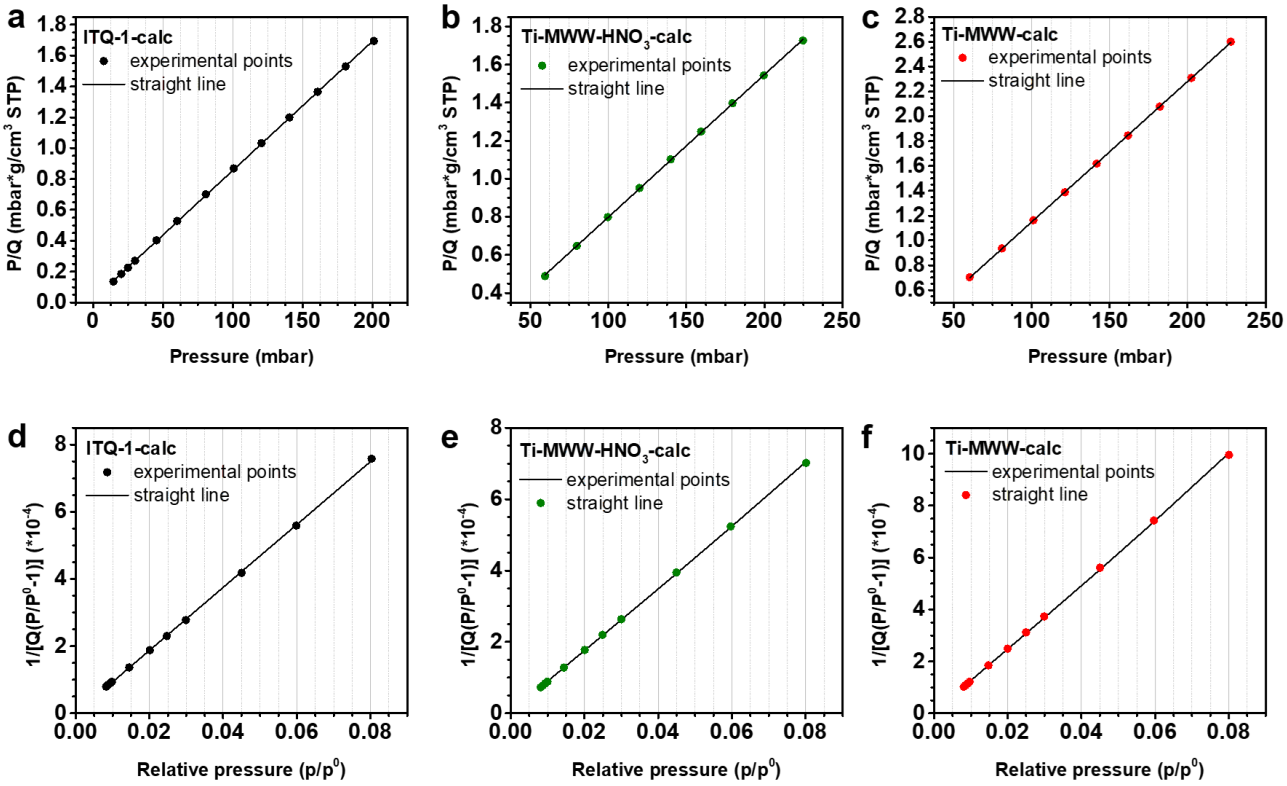

Figure S3. Linearized (a, b, c) Langmuir and (d, e, f) BET fit for N_2 isotherms at -196 °C for the (a, d) ITQ-1 (b, e) Ti-MWW-HNO_3-calc and (c, f) Ti-MWW-calc samples.

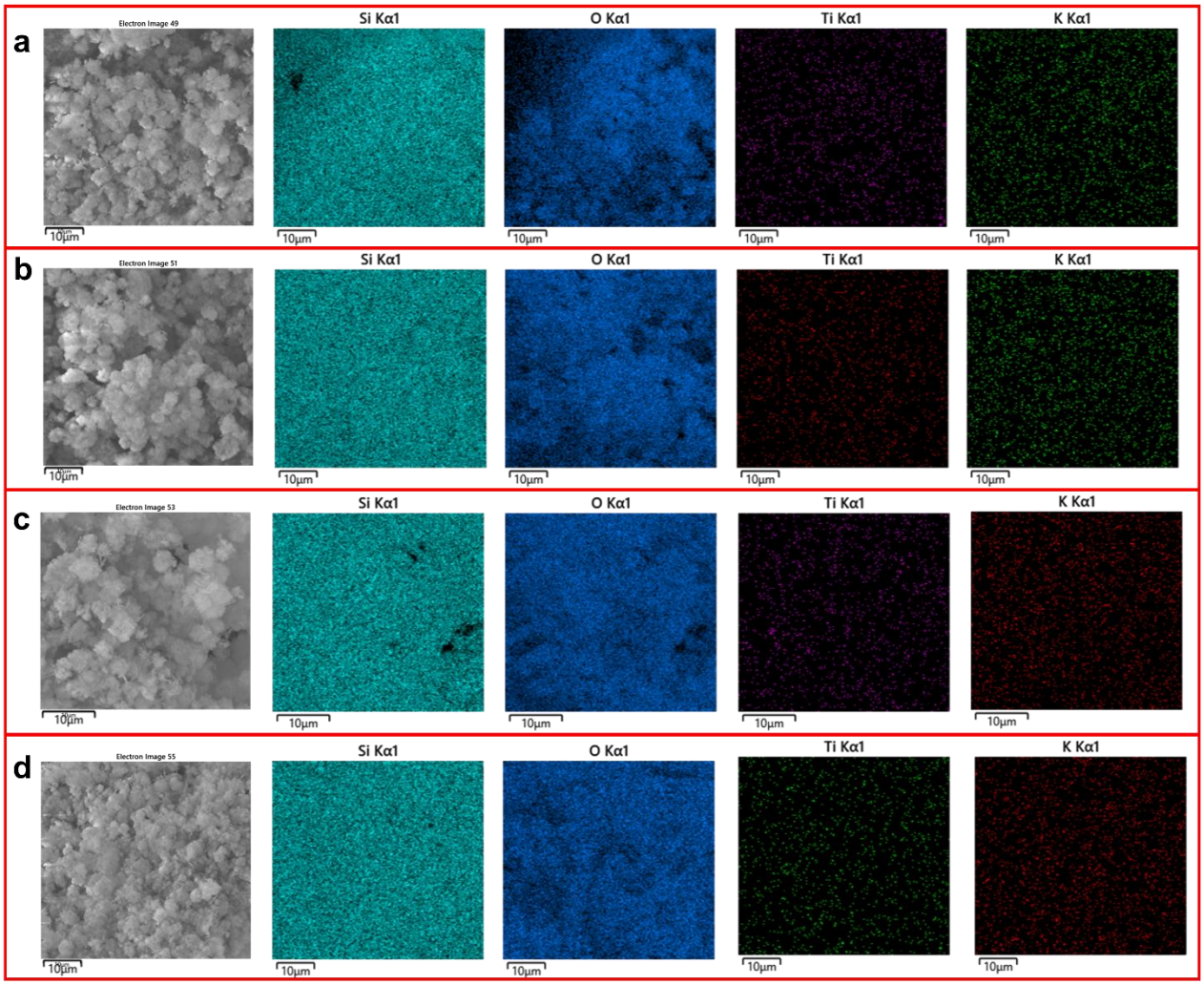

Figure S4. Energy Dispersive X-rays (EDX) Scanning Electron Microscopy (SEM) maps of the four sites used for determination of Ti/Si of Ti-MWW-calc. For each site (a, b, c and d) the SEM image, and the Si, O, Ti and K distribution are shown from left to right.

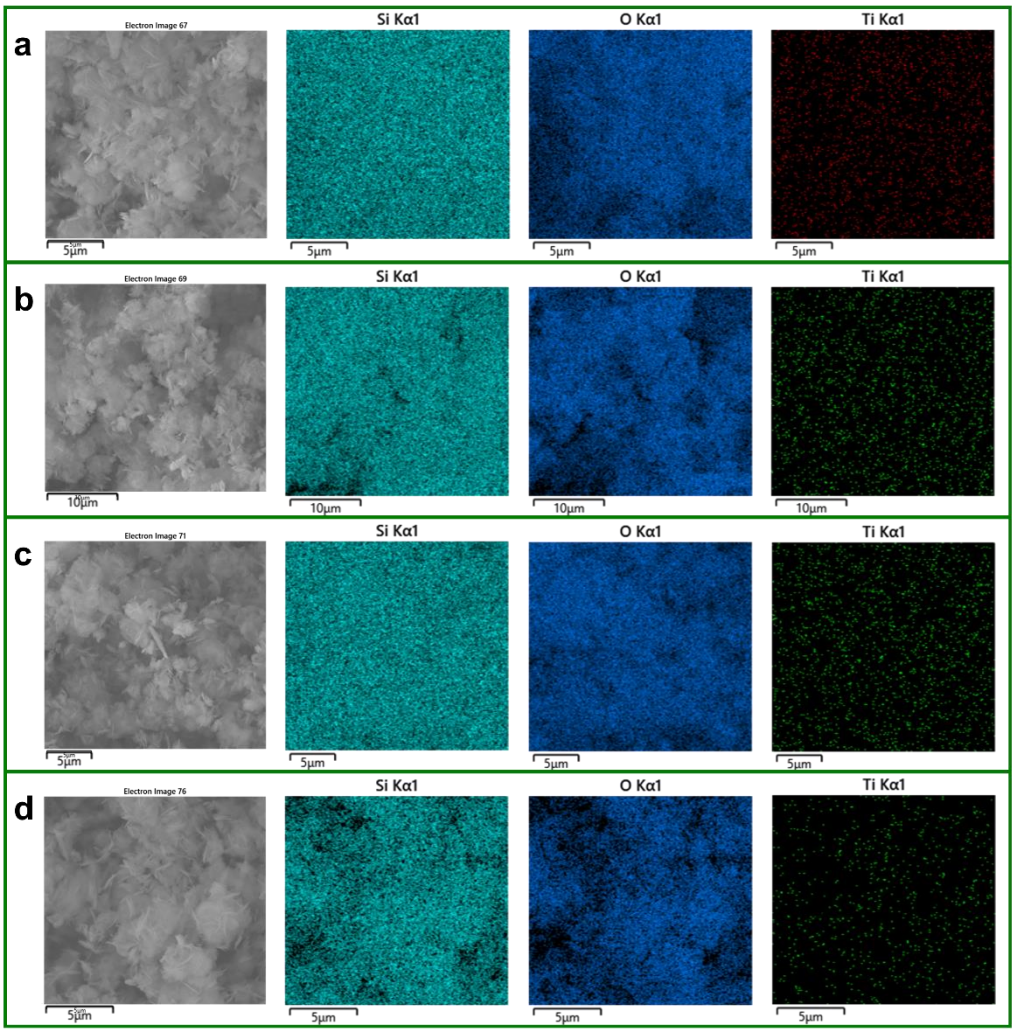

Figure S5. EDX-SEM maps of the four sites used for determination of Ti/Si of Ti-MWW-HNO_3-calc. For each site (a, b, c and d) the SEM image, and the Si, O and Ti distribution are shown from left to right. K is not detected in the sample.

Ti active site characterization

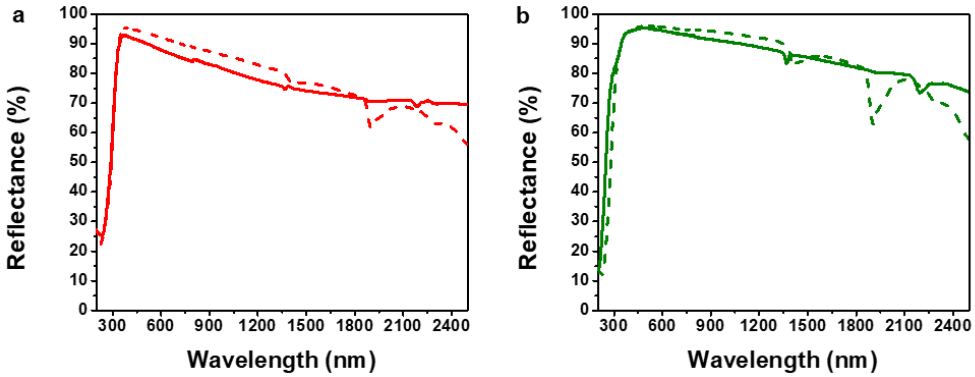

Figure S6. Diffuse Reflectance UV-Vis spectra of (a) Ti-MWW-calc and (b) Ti-MWW-HNO_3-calc, measured "as such" in air (dashed lines) and after outgassing at 500 °C (solid lines).

Figure S7a shows the spectra of Ti-MWW-HNO_3-calc and Ti-MWW-calc samples in Kubelka Munk units for the sake of comprehension and comparison with the UV-Vis spectra commonly published in literature. However, the UV-Vis-NIR spectra reported in the manuscript and in the ESI file of this paper are reported in Reflectance (%) units because the spectra of the samples contacted with H_2O_2 contain very different amount of H_2O. The presence of H_2O in the interparticle voids causes a decrease of the difference between the refraction index of the crystallites and of the void spaces, penalizing the scattering phenomenon. This causes a reduction of the fraction of reflected photons that reach the detector, causing the apparent increase in the sample absorption evident in Figure S7b. When Kubelka Munk units are used, this artifact has a nonlinear magnification, that can be instead correctly evaluated using the Reflectance (%) units.[2]

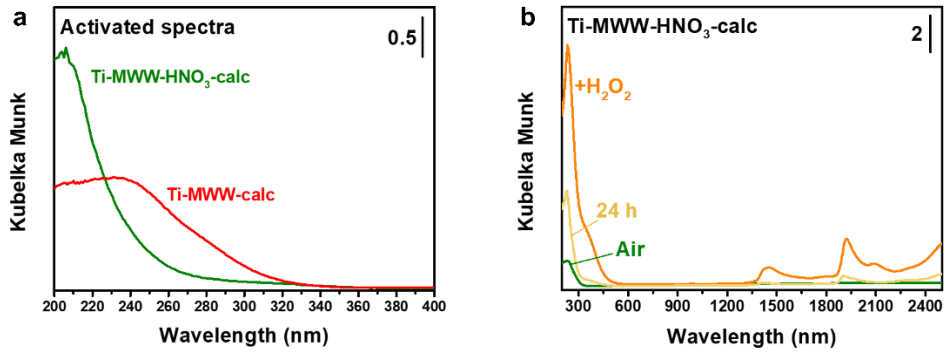

Figure S7. UV-Vis-NIR spectra in DR mode reported in Kubelka Munk units of (a) activated samples Ti-MWW-HNO_3-calc (olive) and Ti-MWW-calc (red) and (b) Ti-MWW-HNO_3-calc after contact with H_2O_2 (+H_2O_2, orange) and dried for 24 h (yellow), respect to the reference Ti-MWW-HNO_3-calc as-such in air (olive).

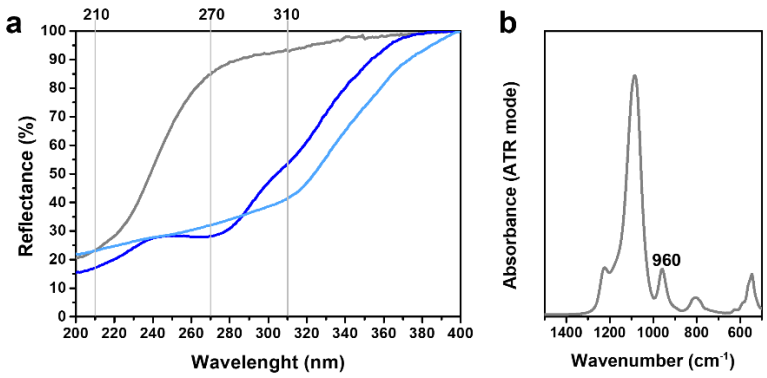

Figure S8. Ti characterization of reference TS-1 samples, whose extended characterization is reported herein:[3,4] TS-1A sample containing only Ti in tetrahedral framework positions (gray), TS-1B sample containing Ti in tetrahedral and amorphous positions (blue) and TS-1C sample containing Ti in tetrahedral and amorphous positions and bulk anatase (light blue). (a) UV-Vis spectra of the samples recorded after activation and (b) ATR-IR spectrum of TS-1A sample recorded after activation.

Study of acid sites and hydroxyls group using probe molecules

Figure S9 shows the background subtracted spectra of carbon monoxide (CO) dosed on Ti-MWW-HNO_3-calc (a, b) and ITQ-1-calc (c, d) at ≈ -173 °C.[5–7] CO is a probe molecule with very low proton affinity (PA(CO) = 141.9 kcal/mol),[7,8] and for this reason it is not able to interact with Ti(IV) sites in tetrahedral coordination, with weak Lewis acidity. For this reason, this experiment was performed to possibly detect differences between the hydroxyl population of the two samples (consisting of both Si-OH and Ti-OH groups, not distinguishable due to their very similar stretching frequency and to the low amount of Ti-OH sites).[3] The spectra in Figure S9 show that no clear differences are present between the Ti-containing and -free samples. In both cases, CO interacts with internal isolated and terminal OH groups *via* H-bonds, originating the erosion of the envelope of bands centered at 3733 cm^{-1} and the formation of the broad band at 3650 cm^{-1} in the hydroxyl spectral region (Figure S9a, c).[7] In the CO stretching region, two bands are present, centered at 2137 and 2156 cm^{-1}. They are assigned to weakly physisorbed and H-bonded CO molecules. As for TS-1, it is not possible to distinguish between Si-OH and Ti-OH groups because of their very similar stretching frequency.[3] The fate of the new band centered at 3688 cm^{-1} in Ti-MWW-HNO_3-calc spectrum is not clear. As highlighted in Figure S10, CO interacts with these sites, but no specific bands grow distinguishable from the broad envelope centered at 3650 cm^{-1}. Finally, the adsorption of CO on both Ti-containing and -free samples is totally reversible at the temperature of the experiment.

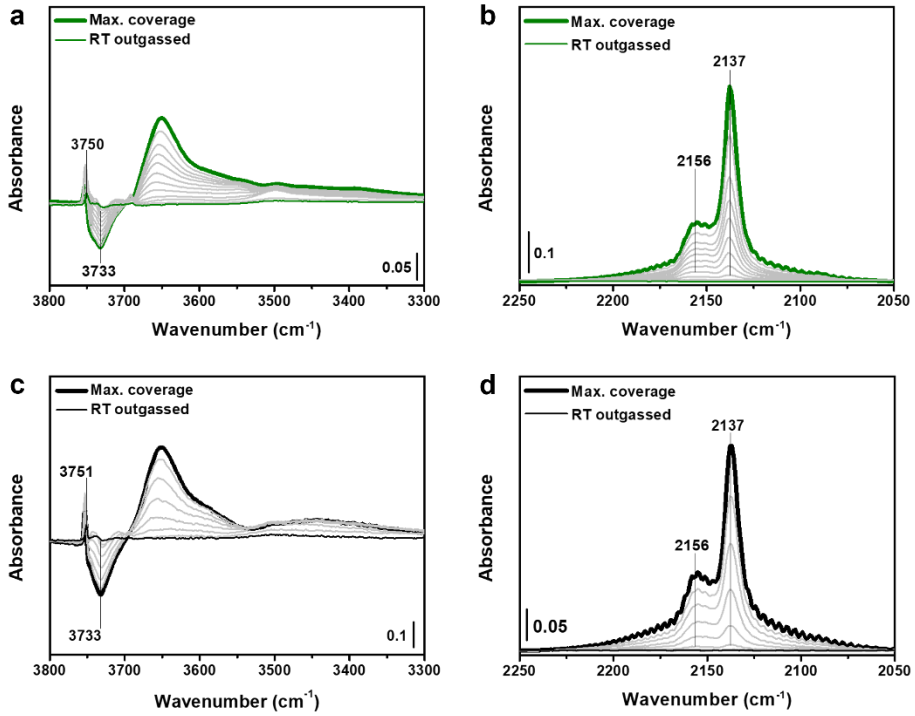

Figure S9. Background subtracted IR spectra of (a, b) Ti-MWW-HNO_3-calc, and (c, d) ITQ-1-calc after contact with CO at -173 °C in the (a, c) 3800-3300 cm^{-1} and (b, d) 2250-2050 cm^{-1} spectral regions. The spectrum of the samples measured after outgassing at 500 °C was used as background.

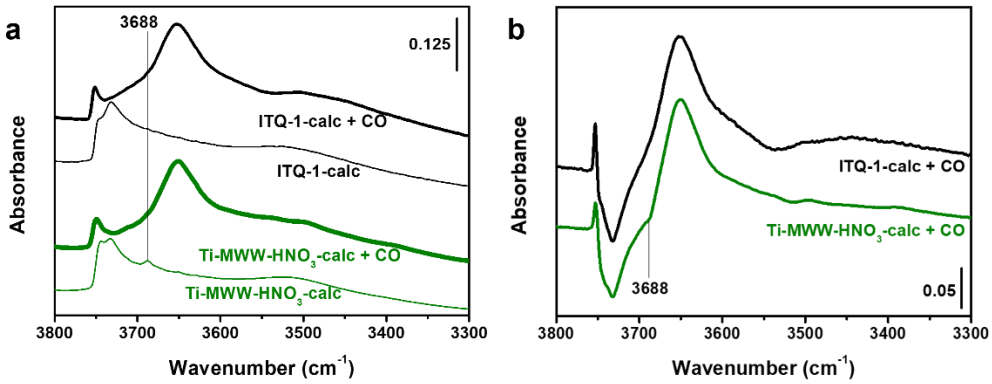

Figure S10. (a) Vertically shifted IR spectra of from bottom to top, activated Ti-MWW-HNO_3-calc, Ti-MWW-HNO_3-calc after CO dosing, activated ITQ-1-calc and ITQ-1-calc after CO dosing and (b) background subtracted IR spectra of (from bottom to top) Ti-MWW-HNO_3-calc and ITQ-1-calc after CO dosing (activated spectra used as background), in the 3800-3300 cm^{-1} spectral region.

Figure S11 shows the background subtracted spectra of pyridine (Py) dosed on Ti-MWW-HNO_3-calc and on the reference ITQ-1. The interpretation of the CH stretching region (3200-3000 cm^{-1}, Figure S11a, c) is affected by the overlap with the broad signal of the hydroxyl groups interacting with Py and by the formation of Evans transparency windows due to the Fermi resonance.[9] In the 1650-1350 cm^{-1} range (Figure S11b, d),

different signals appear after the interaction with Py. These vibrations are assigned to the 8a, 8b, 19a and 19b ring modes of Py.[9] Table S1 summarizes the frequencies of these spectral modes when the Py is physisorbed, perturbed by the interaction via H-bond with Si(Ti)-OH groups and by the formation of Ti(IV)---Py adducts.[9,10] It is noticeable that no band associated to Brønsted acid sites strong enough to protonate Py are present (around 1550 cm^{-1}) and that the band associated to the formation of the Ti(IV)---Py adduct is more resistant to outgassing at RT respect to the bands associated to Si(Ti)-OH sites.

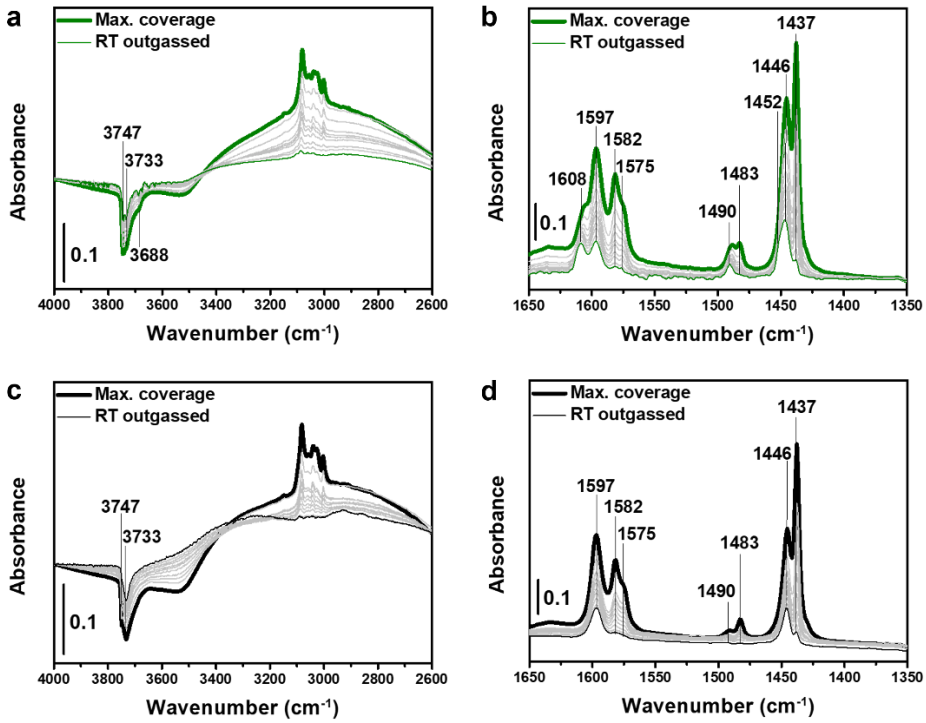

Figure S11. Background subtracted IR spectra of (a, b) Ti-MWW-HNO_3-calc and (c, d) ITQ-1-calc after contact with Py in the regions (a, c) 4000-2600 cm^{-1} and (b, d) 1650-1350 cm^{-1}. The spectrum of the sample after outgassing at 500 °C was used as background.

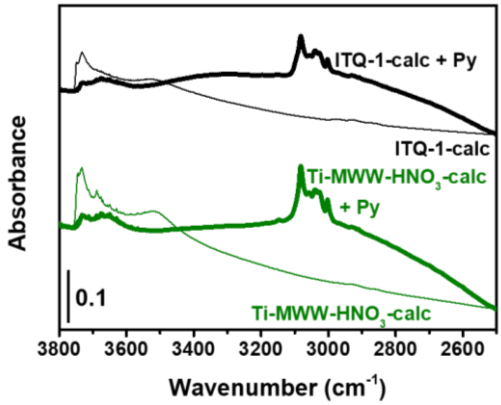

Figure S12. Vertically shifted IR spectra of from bottom to top, activated Ti-MWW-HNO_3-calc, Ti-MWW-HNO_3-calc after Py dosing, activated ITQ-1-calc and ITQ-1-calc after Py dosing. The spectra are vertically shifted for the sake of comparison.

Table S1. Vibrational frequencies and assignment of the bands highlighted in Figure S11b (sh=shoulder).

Wavenumber (cm^{-1})	Specie	Vibration mode	Reference
1597	Si-OH---Py	8a	[9,10]
1582	Si-OH---Py	8b	[9,10]
1490	Si-OH---Py	19a	[9,11]
1446	Si-OH---Py	19b	[9,10]
1608	Ti(IV)---Py	8a	[9]
1490	Ti(IV)---Py	19a	[9]
1452 sh	Ti(IV)---Py	19b	[9]
1597	Physisorbed Py	8a	[9]
1582	Physisorbed Py	8b	[9,10]
1483	Physisorbed Py	19a	[9,11]
1438	Physisorbed Py	19b	[9]

Figure S13 shows the background subtracted (a, c) and as-such (b, d) IR spectra of Ti-MWW-HNO_3-calc (a, b) and ITQ-1-calc (c, d) recorded after contact with ammonia (NH_3) and upon outgassing at RT. NH_3 is the stronger base used as probe molecule in this study. It interacts with all the silanols species present in the samples, determining the erosion of the signals between 3800 and 3100 cm^{-1} and a parallel growth of the broad band centered around 2880 cm^{-1} or 2845 cm^{-1} in Ti-MWW-HNO_3-calc and ITQ-1-calc respectively. Superimposed to this envelope, the sharp symmetric stretching (ν_s) of the NH_3 in gas phase is present, at 3335 and 3333 cm^{-1} in Ti-MWW-HNO_3-calc and ITQ-1-calc respectively; the signal due to the antisymmetric stretching (ν_a) should be at 3444 cm^{-1}, but it is not visible in our spectra and it is probably superimposed to the broad band at 3399 cm^{-1}.[12–14] The bands assigned to ν_s and ν_a of NH_3 in interaction with Si(Ti)-OH are visible and downward shifted, at 3316 and 3399 cm^{-1} in Ti-MWW-HNO_3-calc and at 3315 and 3398 cm^{-1} in ITQ-1-calc respectively.[12–14] In the hydroxyls stretching region of Ti-MWW-HNO_3-calc (inset of Figure S13a-c,

3800-3500 cm^{-1}), upon desorption of NH_3, the growth of a transient band is observed at 3670 cm^{-1}, that is completely eroded at the end of the RT outgassing. Regarding the interaction with the Ti(IV) in tetrahedral coordination, the interaction of NH_3 with the Lewis sites in Ti-MWW-HNO_3-calc produces a perturbation of the ν_s and ν_a of NH_3 (signals at 3296 cm^{-1} and broad band at 3399 cm^{-1}, for the formation of the Ti(IV)---NH_3 complex) and of the asymmetric bending of the NH_3 molecule (at 1609 cm^{-1}, gas phase at 1627 cm^{-1}, in interaction with Si-OH at 1636 cm^{-1}).[12–14] In the framework vibration region, the perturbation of the bands at 930 and 965 cm^{-1} is clearly visible. They upward shift to 940 and 975 cm^{-1} respectively. This is the final confirmation that the band at 965 cm^{-1} is mainly due to tetrahedral Ti sites, more than to defective Si-OH sites, that vibrate at the same frequency.[14] Two sharp signals, superimposed to the framework vibration bands, grow at 966 and 931 cm^{-1} in both samples at high NH_3 coverage. They are due to $\nu_2(a_1)$ vibration of the gas phase NH_3 and completely disappear after the first outgassing step. [12]

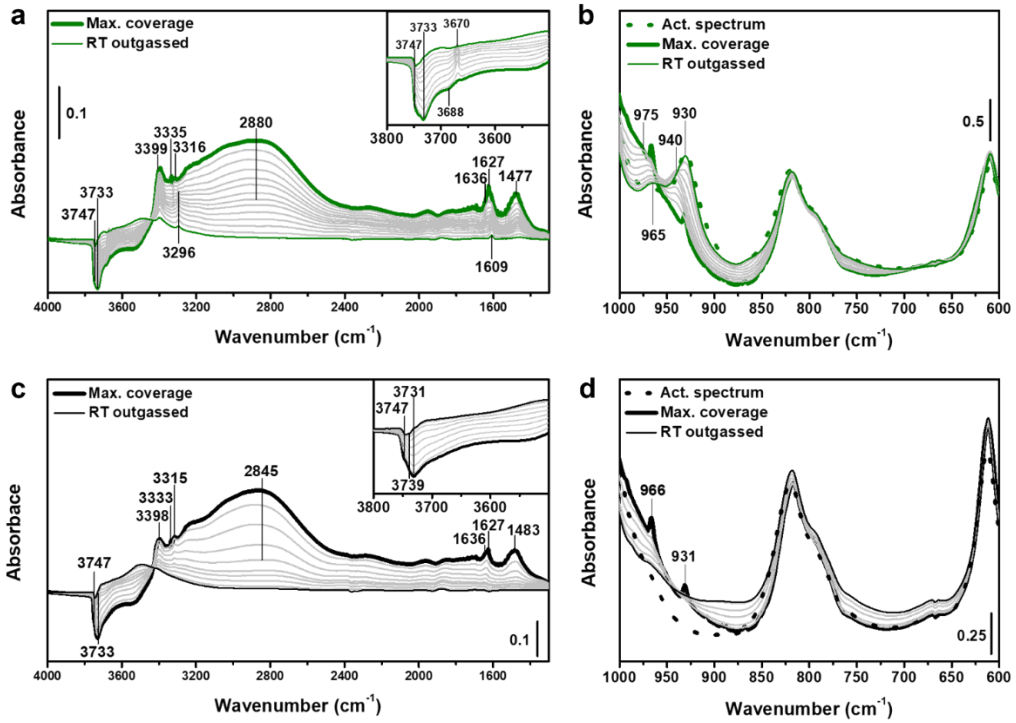

Figure S13. Background subtracted IR spectra of (a) Ti-MWW-HNO_3-calc and (c) ITQ-1-calc after contact with NH_3 at RT, in the 4000-1300 cm^{-1} spectral region. The spectrum of the sample after outgassing at 500 °C was used as background. IR spectra of (b) Ti-MWW-HNO_3-calc and (d) ITQ-1-calc after contact with NH_3 in the framework vibration region (1000-600 cm^{-1}).

Study of the interaction with H_2O_2

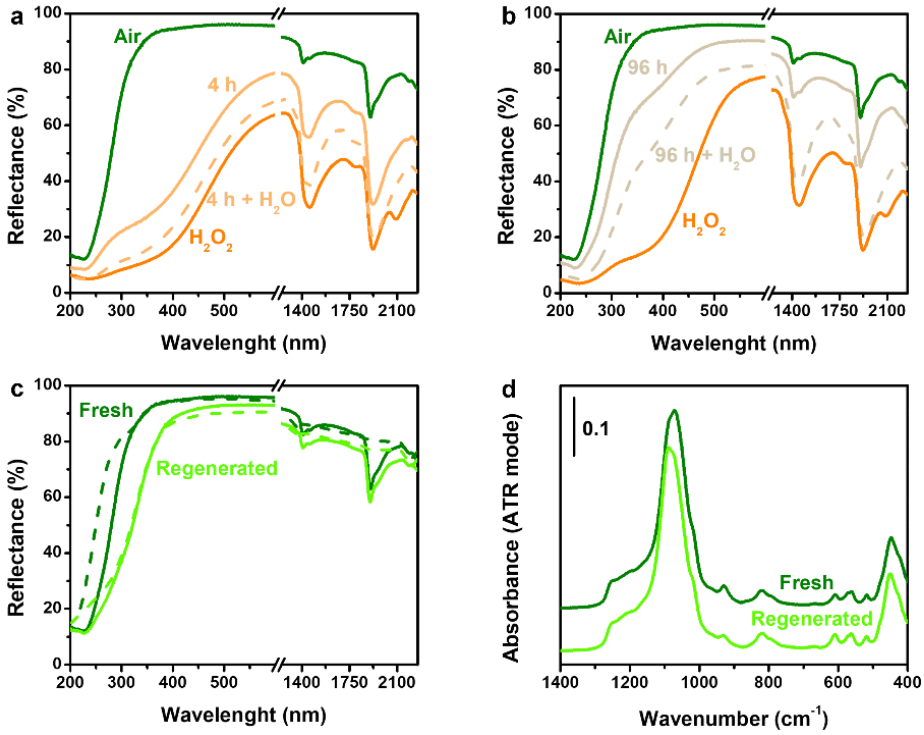

Figure S14. (a) UV-Vis-NIR spectra of Ti-MWW-HNO_3-calc in air (olive), contacted with H_2O_2 (orange), dried for 4 h (full light salmon) and further contacted with H_2O (dashed light salmon). (b) UV-Vis-NIR spectra of Ti-MWW-HNO_3-calc in air (olive), contacted with H_2O_2 (orange), dried for 96 h (full ocher) and further contacted with H_2O (dashed ocher). (c) UV-Vis-NIR spectra of fresh Ti-MWW-HNO_3-calc in air (full olive), after activation (dashed olive) and after two cycles with H_2O_2 and calcination (regeneration), in air (full light green) and after activation (dashed light green). (d) Activated ATR-IR spectra of Ti-MWW-HNO_3-calc of the fresh sample (olive) and of the regenerated sample after two cycles in contact with H_2O_2 and calcination (light green).

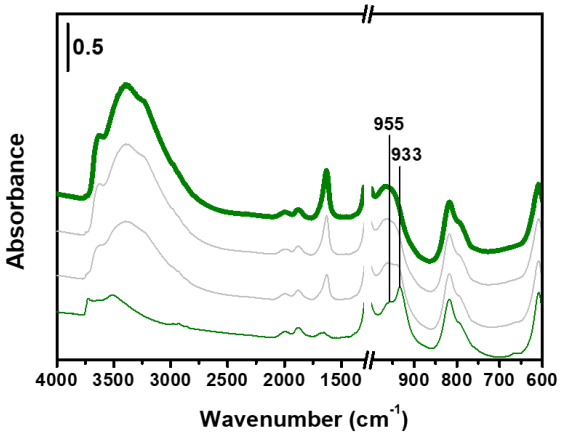

Figure S15. Transmission IR spectra of Ti-MWW-HNO_3-calc recorded during outgassing at RT: progressive outgassing from top (bold olive line) to bottom (olive line). The spectra are vertically shifted for the sake of clarity.

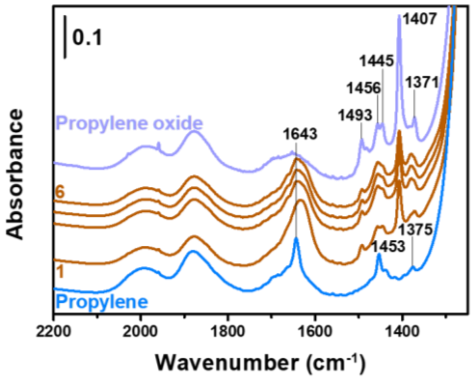

Figure S16. Transmission IR spectra in the 2200-1250 cm^{-1} spectral range of (from bottom to top) pure propylene dosed on RT outgassed Ti-MWW-HNO_3-calc (blue), pure propylene dosed on H_2O_2 soaked and RT outgassed Ti-MWW-HNO_3-calc (dark orange, from 1 to 6 evolution in time: 1 recorded immediately afterwards dosing propylene and from 2 to 6 one spectrum per minute) and pure propylene oxide dosed on RT outgassed Ti-MWW-HNO_3-calc (light purple).

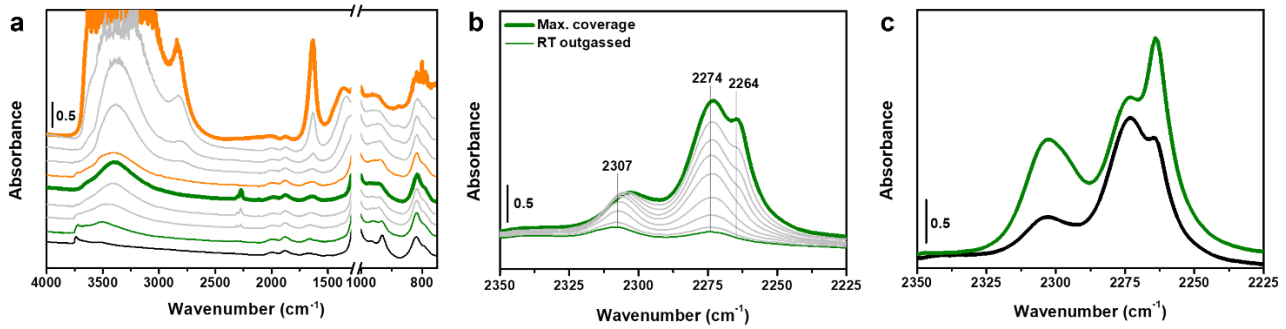

Figure S17. Transmission IR spectra of (a) Ti-MWW-HNO_3-calc (the activated spectrum is reported in black) after H_2O_2 soaking and rapid outgassing (from bold orange to orange) and successive CD_3CN dosage and progressive outgassing (from bold olive to olive), in the 2500-750 cm^{-1} spectral range (the spectra are vertically shifted for the sake of comparison), (b) CN stretching mode spectral range of spectra sequence from bold olive to olive and (c) comparison of a saturation dose of CD_3CN adsorbed on Ti-MWW-HNO_3-calc after activation, as in Figure 4b (olive) and on Ti-MWW-HNO_3-calc after H_2O_2 soaking and rapid outgassing as in panel b.

References

(1) Rosso, F.; Airi, A.; Signorile, M.; Dib, E.; Bordiga, S.; Crocellà, V.; Mintova, S.; Bonino, F. Insight on MWW Siliceous Zeolites: From 2D Precursors toward 3D Structure. *Microporous Mesoporous Mater.* **2023**. https://doi.org/10.2139/ssrn.4612019.

(2) Bonino, F.; Damin, A.; Ricchiardi, G.; Ricci, M.; Spanò, G.; D'Aloisio, R.; Zecchina, A.; Lamberti, C.; Prestipino, C.; Bordiga, S. Ti-Peroxo Species in the TS-1/H_2O_2/H_2O System. *J. Phys. Chem. B* **2004**, *108* (11), 3573–3583. https://doi.org/10.1021/jp036166e.

(3) Signorile, M.; Crocellà, V.; Damin, A.; Rossi, B.; Lamberti, C.; Bonino, F.; Bordiga, S. Effect of Ti Speciation on Catalytic Performance of TS-1 in the Hydrogen Peroxide to Propylene Oxide Reaction. *J. Phys. Chem. C* **2018**, *122* (16), 9021–9034. https://doi.org/10.1021/acs.jpcc.8b01401.

(4) Signorile, M.; Braglia, L.; Crocellà, V.; Torelli, P.; Groppo, E.; Ricchiardi, G.; Bordiga, S.; Bonino, F. Titanium Defective Sites in TS-1: Structural Insights by Combining Spectroscopy and Simulation. *Angew. Chem. Int. Ed.* **2020**, *59* (41), 18145–18150. https://doi.org/10.1002/anie.202005841.

(5) Bordiga, S.; Roggero, I.; Ugliengo, P.; Zecchina, A.; Bolis, V.; Artioli, G.; Buzzoni, R.; Marra, G.; Rivetti, F.; Spano, G.; Lamberti, C. Characterisation of Defective Silicalites. *J. Chem. Soc. Dalton Trans.* **2000**, 21, 3921–3929. https://doi.org/10.1039/b004794p.

(6) Zecchina, A.; Bordiga, S.; Spoto, G.; Marchese, L.; Petrini, G.; Leofanti, G.; Padovan, M. Silicalite Characterization. 2. IR Spectroscopy of the Interaction of CO with Internal and External Hydroxyl Groups. *J. Phys. Chem.* **1992**, *96* (12), 4991–4997. https://doi.org/10.1021/j100191a048.

(7) Busca, G. Acidity and Basicity of Zeolites: A Fundamental Approach. *Microporous Mesoporous Mater.* **2017**, *254*, 3–16. https://doi.org/10.1016/j.micromeso.2017.04.007.

(8) Bordiga, S.; Lamberti, C.; Bonino, F.; Travert, A.; Thibault-Starzyk, F. Probing Zeolites by Vibrational Spectroscopies. *Chem. Soc. Rev.* **2015**, *44* (20), 7262–7341. https://doi.org/10.1039/c5cs00396b.

(9) Bonino, F.; Damin, A.; Bordiga, S.; Lamberti, C.; Zecchina, A. Interaction of CD_3CN and Pyridine with the Ti(IV) Centers of TS-1 Catalysts: A Spectroscopic and Computational Study. *Langmuir* **2003**, *19* (6), 2155–2161. https://doi.org/10.1021/la0262194.

(10) Buzzoni, R.; Bordiga, S.; Ricchiardi, G.; Lamberti, C.; Zecchina, A.; Bellussi, G. Interaction of Pyridine with Acidic (H-ZSM5, H-, H-MORD Zeolites) and Superacidic (H-Nafion Membrane) Systems: An IR Investigation. *Langmuir* **1996**, *12*, 930–940.

(11) Morterra, C.; Cerrato, G.; Visca, M.; Lenti, D. M. IR Surface Characterization of Some TiO_2-Based Pigments. 1. Preparation of Pigmentary Materials. *Chem. Mater.* **1991**, *3*, 132–142.

(12) Gianotti, E.; Dellarocca, V.; Marchese, L.; Martra, G.; Coluccia, S.; Maschmeyer, T. NH_3 Adsorption on MCM-41 and Ti-Grafted MCM-41. FTIR, DR UV-Vis-NIR and Photoluminescence Studies. *Phys. Chem. Chem. Phys.* **2002**, *4* (24), 6109–6115. https://doi.org/10.1039/b207231a.

(13) Bolis, V.; Bordiga, S.; Lamberti, C.; Zecchina, A.; Carati, A.; Rivetti, F.; Spanò, G.; Petrini, G. Heterogeneity of Framework Ti(IV) in Ti - Silicalite as Revealed by the Adsorption of NH_3. Combined Calorimetric and Spectroscopic Study. *Langmuir* **1999**, *15* (18), 5753–5764. https://doi.org/10.1021/la981420t.

(14) Bordiga, S.; Damin, A.; Bonino, F.; Zecchina, A.; Spanò, G.; Rivetti, F.; Bolis, V.; Prestipino, C.; Lamberti, C. Effect of Interaction with H_2O and NH_3 on the Vibrational, Electronic, and Energetic Peculiarities of Ti(IV) Centers TS-1 Catalysts: A Spectroscopic and Computational Study. *J. Phys. Chem. B* **2002**, *106* (38), 9892–9905. https://doi.org/10.1021/jp026106t.